Eur. Phys. J. D **61**, 657–662 (2011)
DOI: 10.1140/epjd/e2010-10246-4

THE EUROPEAN PHYSICAL JOURNAL D

Regular Article

Effect of catalysts on dc corona discharge poisoning

S. Pekárek[a]

Czech Technical University in Prague, Faculty of Electrical Engineering, Technická 2, 16627 Prague 6, Czech Republic

Received 3 May 2010 / Received in final form 15 October 2010
Published online 4 February 2011 –

Abstract. The processes of ozone generation in non-thermal plasma produced by an electrical discharge in air at atmospheric pressure are burdened by the presence of nitrogen oxides, which on the one hand contribute to ozone generation and on the other hand are responsible for unpleasant discharge poisoning. The term discharge poisoning refers to the situation when the discharge ozone formation completely breaks down. Discharge poisoning can be affected by placing a catalyst in the discharge chamber. For the dc hollow needle to mesh corona discharge enhanced by the flow of air through the needle electrode we studied the effect of titanium dioxide TiO_2, ZSM-5 zeolite or Cu^{++}ZSM-5 zeolite on discharge poisoning by monitoring the ozone, nitrogen monoxide and nitrogen dioxide discharge production. We found that placing globules of any of these catalysts on the mesh decreases the energy density of the onset of discharge poisoning, and this energy density is smallest for a discharge with globules of a TiO_2 on the mesh.

1 Introduction

The beneficial properties of ozone for drinking water treatment, sterilization, medicines, storage of food, fruit and vegetables etc. are well known [1]. In many small and medium-size devices, ozone is produced by electrical discharges from air. Ozone generation processes from air start with dissociation, excitation and ionization of oxygen and nitrogen molecules. The main ozone generating reaction dominant at atmospheric pressure is

$$O + O_2 + M \rightarrow O_3^* + M \rightarrow O_3 + M, \quad (1)$$

where M is a third-body collision partner (in air O_2, N_2), or a solid metallic/dielectric surface [2].

In the case of ozone generation from air, the existence of nitrogen molecules causes the appearance of various types of positive nitrogen ions, nitrogen atoms and excited atomic and other molecular species [3,4], which on the one hand produce additional oxygen atoms for ozone generation but, on the other hand, cause discharge poisoning [5,6]. The term discharge poisoning refers to the situation when discharge ozone formation completely breaks down. Under such conditions, neither ozone nor N_2O_5 appears in the product gas, and NO, NO_2 and N_2O can be detected instead. This state is characterized by rapid NO_x reactions consuming oxygen atoms at a faster rate than the ozone formation:

$$O + NO + M \rightarrow NO_2 + M \quad (2)$$
$$O + NO_2 \rightarrow NO + O_2 \quad (3)$$
$$O + O \rightarrow O_2. \quad (4)$$

The result is an accelerated catalytic recombination of oxygen atoms. The previously formed ozone is removed in ozone destruction processes:

$$NO + O_3 \rightarrow NO_2 + O_2 \quad (5)$$
$$O + O_3 \rightarrow 2O_2. \quad (6)$$

Thus the resultant concentration of ozone and nitrogen oxides produced by the discharge represents a dynamic balance of ozone formation and also its destruction reactions.

Until now, the attention of researchers has been mainly focused on improving discharge ozone production with the help of catalysts [7–12]. The basic idea behind our research was to affect the discharge nitrogen oxides and ozone production by placing various catalysts in the discharge region in order to influence the onset of the discharge poisoning. The discharge poisoning is an important phenomenon, with a direct impact on functioning of ozone generating devices.

The first catalyst that we tested was titanium dioxide. The TiO_2 is a catalyst, which is used to enhance discharge ozone production, to decompose volatile organic compounds; it is used in air purification devices, in water treatment, water purification, deodorizing, etc. This photocatalyst is n-type semiconductor, which can be activated by the UV radiation emitted by the discharge.

Since the presence of nitrogen monoxide and nitrogen dioxide plays a decisive role in discharge poisoning, we attempted to find a catalyst that decomposes these oxides. Indeed, decomposition or reduction of nitrogen monoxide is a major target for industries using high temperature combustion. The catalysts tested for nitrogen oxides decomposition are zeolites [13–20] and mainly copper-ion

[a] e-mail: pekarek@fel.cvut.cz

exchanged ZSM-5 zeolites [15–20]. A zeolite is an inorganic porous material having a highly regular structure of pores and chambers that allows some molecules to pass through, and causes others to be either excluded or broken down. Generally, zeolites exhibit no measurable electronic conductivity since they have a wide electronic band gap of several electronvolts. For their activation can be in some cases used the increased temperature [16,17], and in some cases the UV radiation [13,18–20].

We therefore decided to affect the production of discharge nitrogen oxides with the ZSM-5 zeolite, which is an aluminosilicate zeolite with high silica and low alumina content. The second zeolite tested here was copper-ion exchanged Cu^{++}ZSM-5.

Because of its relative simplicity, for our experiments we used a hollow needle to mesh dc corona discharge enhanced by the flow of air through the needle electrode.

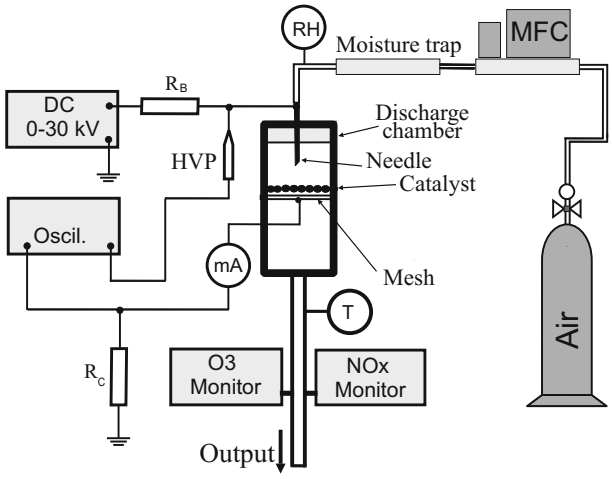

Fig. 1. Experimental arrangement. *RH* – relative humidity sensor, *MFC* – mass flow controller, *T* – thermometer, R_B – ballast resistor, R_C – earthed resistor.

2 Experimental arrangement

The experimental arrangement is shown in Figure 1. The electrodes – a stainless steel hollow needle and a stainless steel mesh situated perpendicular to the needle – were situated in a circular glass discharge chamber with an inner diameter of 32 mm. The needle had an inner diameter of 0.7 mm and an outer diameter of 1.2 mm. The tip of the needle was sharpened at an angle of 15°. The mesh had rhombus cells with dimensions of 0.60×0.50 mm and thickness 0.15 mm. The distance between the tip of the needle and the mesh was adjusted to $d = 8.1$ mm. This distance was chosen on the basis of preliminary experiments with the production of nitrogen oxides, so that the detected values of these oxide concentrations for chosen distance d fitted within the measuring range of the NO_x monitor.

Air from a cylinder was supplied to the needle through a Hydro-Purge II moisture trap. A mass flow controller, *MFC*, adjusted the air flow through the needle. The relative humidity *RH* of the air was measured at the input of the discharge chamber. We also measured the temperature T of the air at the output. A fan cooled the discharge tube.

The Technix regulated dc high-voltage power supply provided voltage up to 30 kV. The needle, biased negatively, was ballasted by a resistor R_B.

The ozone concentration was measured by absorption of the 254 nm UV spectral line, using an API 450 ozone monitor.

The concentration of nitrogen oxides was measured using a GA-60 toxic gases monitor. This monitor was equipped with 5 electrochemical cells to measure the concentrations of nitrogen monoxide, nitrogen dioxide, oxygen, carbon dioxide, and sulphur dioxide. The measuring range for nitrogen monoxide concentration was 0 to 5000 ppm, and the range of nitrogen dioxide concentration was 0 to 800 ppm. This monitor was calibrated for these two oxides using mixtures of various concentrations of nitrogen monoxide or nitrogen dioxide in synthetic air.

The mean value of the discharge current I was determined in two ways. First, we used the value obtained from the magneto-electric system milliammeter. In the second case, the current was determined as the mean value of the signal obtained from the voltage drop on the earthed resistor R_C. This signal was recorded on the first channel of the DS 1150C digital oscilloscope (bandwidth 150 MHz). The discharge voltage U was determined as the mean value of the signal recorded on the second channel of this oscilloscope through a high voltage probe (HVP-28HF, Pintek, division ratio 1000/1, frequency up to 200 MHz).

It should also be mentioned that the discharge in the streamer regime is a strong emitter of electromagnetic noise [21,22], which influences the functioning of the oscilloscope, the nitrogen oxides monitor and the communication line between the oscilloscope and the computer. To reduce the effect of this noise on these devices and to enable correct measurement of voltage and current, the discharge chamber was placed into a Faraday cage, the wires were shielded and the GA-60 monitor, the oscilloscope and the computer were battery-operated.

The experiments were performed with globules of three different catalysts, which were placed on the mesh. The first catalyst to be tested was titanium dioxide TiO_2 photocatalyst Aerolyst 7706. The cylindrical globules were ∼3 mm in diameter and ∼4 mm in height. The ZSM-5 zeolite was in the form of irregular spheres of whitish color ranging in diameter between 1 mm and 2 mm. The cylindrical globules of Cu^{++}ZSM-5 zeolite of bluish color were of similar dimensions as the globules of TiO_2 (∼3 mm in diameter and between 3 mm and 4 mm in height).

3 Experimental results and discussion

All experiments were performed with the distance between the tip of the needle and the mesh $d = 8.1$ mm, flow of air through the needle $Q = 1.8$ slm, and relative humidity of air $RH = 0.8\%$. The experimental results presented in

following figures are the average values obtained from four measurements.

To compare the results dealing with production of ozone and nitrogen oxides for discharge with a simple mesh and for discharge with globules of various catalysts on the mesh, it is necessary to take into account several facts. First of all placing different catalysts on the mesh changes the electrical characteristics of the discharge in various ways. To include this fact into the analysis of the results, we present the concentrations of ozone and nitrogen oxides as a function of the energy density. The energy density is defined as the ratio of the mean power delivered to the discharge and the flow of the air through the needle electrode. The second aspect is related to the shape, dimensions and masses of particular catalysts globules. Therefore all presented results are valid for experimental conditions mentioned in figures captions.

3.1 Electrical characteristics of the discharge

The processes of ozone and nitrogen oxides formation and destruction are closely connected with electrical parameters of the discharge. Thus the dissociation rate coefficients of O_2 and N_2 depend on the energy distribution of the electrons in the discharge. These coefficients are usually treated as functions of a reduced electric field (E/n), which depends on the discharge voltage. In addition, the electron density in the discharge is controlled by the discharge current. Obviously the electrical parameters of the discharge affect the formation and destruction processes of ozone and nitrogen oxides. The volt-ampere characteristics of the discharge for the needle to mesh electrodes and these electrodes with a layer of globules of TiO_2, ZSM-5 or Cu^{++}ZSM-5 on the mesh are shown in Figure 2.

The dc corona discharge depending on the value of the current can exist in different regimes [23,24]. For the low current region, which in our case corresponds to the discharge in the Trichel pulses regime and in the pulseless glow regime, the discharge voltage increases with increasing current. For the higher current region, which corresponds to the discharge in the filamentary streamer regime, the discharge voltage decreases with increasing current. The transition between these two regimes occurs when the discharge voltage exceeds its maximum, and the corresponding current is labeled as the transition current I_{tr}. Figure 2 shows that the transition current between the diffusive glow regime and the filamentary streamer regime for a discharge with a simple mesh is $I_{tr1} \sim 0.30$ mA, the transition current for a discharge with a layer of TiO_2 is $I_{tr2} \sim 0.35$ mA, the transition current for a discharge with a layer of Cu^{++}ZSM-5 on the mesh is $I_{tr3} \sim 0.45$ mA and finally the transition current for a discharge with a layer of ZSM-5 zeolite on the mesh is $I_{tr4} \sim 0.50$ mA. We can therefore conclude that placing any of the investigated catalysts on the mesh shifts the transition current I_{tr} to higher values. This finding is in agreement with our previous results dealing with the TiO_2 only [24].

In contrast with "packed bed reactors", which use dielectric or ferroelectric pellets in the discharge volume and

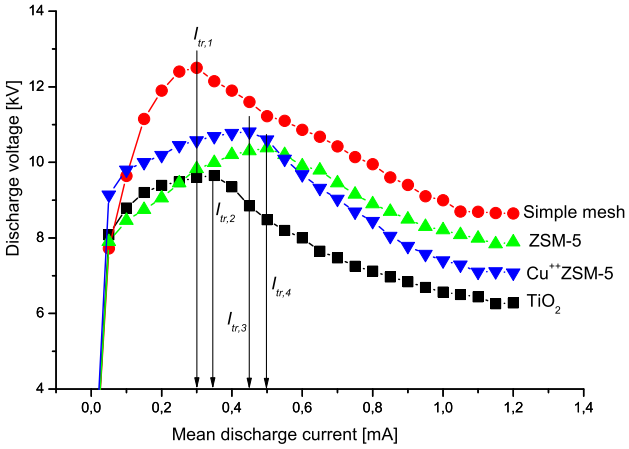

Fig. 2. (Color online) Volt-ampere characteristics for the discharge with the needle to the mesh electrodes; needle to the mesh electrodes with TiO_2; with ZSM-5, or with Cu^{++}ZSM-5. Needle negative, $d = 8.1$ mm, $Q = 1.8$ slm, $RH = 0.8\%$. Mass of TiO_2 globules $m = 0.7691$ g, mass of ZSM-5 $m = 0.5203$ g, mass of Cu^{++}ZSM-5 $m = 0.5398$ g.

ac or pulse discharge energetization we investigated dc corona discharge in which were placed globules of a semiconductor or an insulator on the mesh electrode. This certainly leads to different discharge mechanism – in case of "packed bed reactors" it is the enhancement of electric field. On the other hand in case of the dc discharge energetization take place the processes associated with different electrical properties of various catalysts. Thus for example, when the catalyst is placed on the mesh, it acts as a "virtual" electrode, and the distance between the needle electrode and the mesh is decreased. This decrease in the discharge voltage when the catalyst is placed on the mesh is shown in Figure 2.

3.2 Ozone, nitrogen monoxide and dioxide concentrations versus energy density

The dependence of ozone or nitrogen monoxide concentration versus energy density for the discharge with a simple mesh electrode and a mesh electrode with a layer of globules of TiO_2, ZSM-5 or Cu^{++}ZSM-5 is shown in Figures 3 and 4 respectively. The energy density of the onset of discharge poisoning is determined as the energy density for which the concentration of ozone produced by the discharge falls to zero, or as the energy density at which nitrogen monoxide appears in the discharge products. The values of energy densities of the onset of discharge poisoning obtained from the ozone concentration measurements coincide with the values obtained from the nitrogen monoxide measurements. The effect of different catalysts on the onset of discharge poisoning is nicely displayed in these two figures.

The energy densities of the onset of discharge poisoning are summarized in Table 1.

The energy density of the onset of discharge poisoning is smallest for the discharge with globules of TiO_2 on the

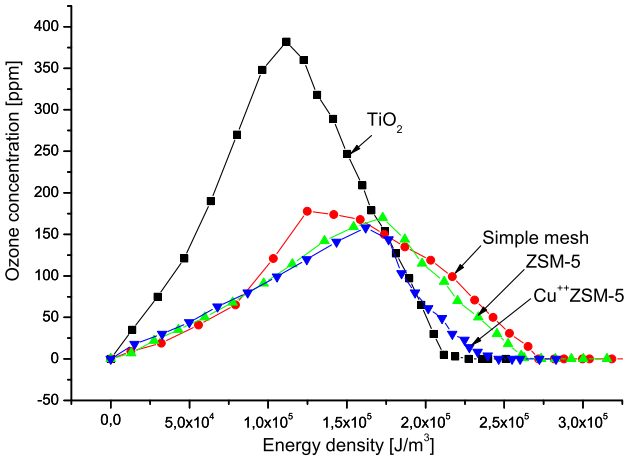

Fig. 3. (Color online) Ozone concentration versus energy density for the discharge with the needle to the mesh electrodes; needle to the mesh electrodes with TiO_2; with ZSM-5, or with Cu^{++}ZSM-5. Needle negative, $d = 8.1$ mm, $Q = 1.8$ slm, $RH = 0.8\%$. Mass of TiO_2 globules $m = 0.7691$ g, mass of ZSM-5 $m = 0.5203$ g, mass of Cu^{++}ZSM-5 $m = 0.5398$ g.

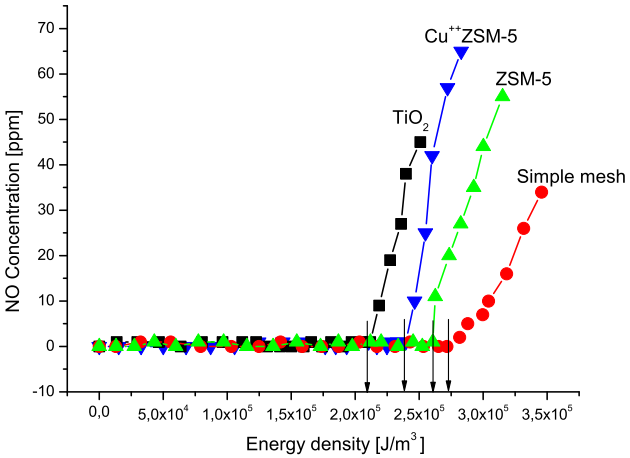

Fig. 4. (Color online) Nitrogen monoxide concentration versus energy density for the discharge with the needle to the mesh electrodes; needle to the mesh electrodes with TiO_2; with ZSM-5, or with Cu^{++}ZSM-5. Needle negative, $d = 8.1$ mm, $Q = 1.8$ slm. $RH = 0.8\%$. Mass of TiO_2 globules $m = 0.7691$ g, mass of ZSM-5 $m = 0.5203$ g and mass of Cu^{++}ZSM-5 $m = 0.5398$ g.

mesh and the highest for the discharge with a simple mesh electrode. Placing any of the investigated catalysts on the mesh decreases the energy density of the onset of discharge poisoning with respect to the discharge with a simple mesh electrode.

The observed different decrease of the onset of discharge poisoning energy density in case when the various catalysts are placed on the mesh can be attributed to different processes contributing in different ways to ozone and nitrogen oxides production.

The smallest energy density of the onset of discharge poisoning was obtained for the discharge with a layer of TiO_2 globules on the mesh. Thus in this case the photoactivation of this catalysts must be, apart of the "classical" ozone and nitrogen oxides production and destruction processes, taken into account. Titanium dioxide is an n-type semiconductor with a series of energy levels associated valence band and a second series of spatially diffuse higher energy levels associated with conduction band. These bands are separated by a forbidden energy gap of 3.2 eV, which corresponds to the wavelength 388 nm. Incidence of UV radiation of a wavelength equal or smaller than 388 nm can promote electrons from the valance band to the largely vacant conduction band. Simultaneously, a positive hole with strong oxidizing capability is formed.

Table 1.

	Energy density of the onset of discharge poisoning (J/m^3)
Mesh with a layer of TiO_2 globules	$\sim 2.09 \times 10^5$
Mesh with a layer of Cu^{++}ZSM-5 globules	$\sim 2.38 \times 10^5$
Mesh with a layer of ZSM-5 globules	$\sim 2.61 \times 10^5$
Simple mesh	$\sim 2.73 \times 10^5$

The corona discharge in air is a strong emitter of UV radiation [22,25–28]. The strongest ultraviolet emission originates from the second positive system of nitrogen ($C_3\Pi_u \rightarrow B_3\Pi_g$), which emits radiation of wavelength 337.1 nm [26]. The first negative system ($B_2\Sigma_u^+ \rightarrow X_2\Sigma_g^+$) of N_2^+, emits radiation of wavelength 391.4 nm. Taking into account the wavelengths of UV radiation required for TiO_2 photoactivation it is therefore seen that corona discharge UV emission could be used for this purpose. The electron and positive hole then can react with the molecules in the vicinity of the catalyst. In air, the electron reacts with an oxygen molecule to form the superoxide anion O_2^-. This anion and other radicals contribute differently to the processes leading to discharge ozone production. As far as in case of negative corona discharge in air the current is sustained by negative ions, the appearance of superoxide anions due to the TiO_2 photoactivation also contribute to the discharge current and therefore to the change of discharge electrical characteristics.

The second smallest energy density of the onset of discharge poisoning was obtained for the discharge with a layer of Cu^{++}ZSM-5 globules on the mesh. In this case the mechanism of NO decomposition associated with adsorption on the surface of this zeolite must be taken into account. This mechanism is based on active sites consisting of coordinately unsaturated cupric (Cu^{++}) ions. These sites are posited to chemisorb NO molecules. The pair of absorbed NO molecules then desorbs as N_2 and O_2. Apart of this in the case of Cu^{++}ZSM-5 zeolite it was found that its UV irradiation of wavelength around 300 nm in the presence of NO leads to decomposition of NO into N_2 and O_2 at temperatures as low as 275 K [18,19].

Higher energy density of the onset of discharge poisoning was obtained for the discharge with a layer of ZSM-5

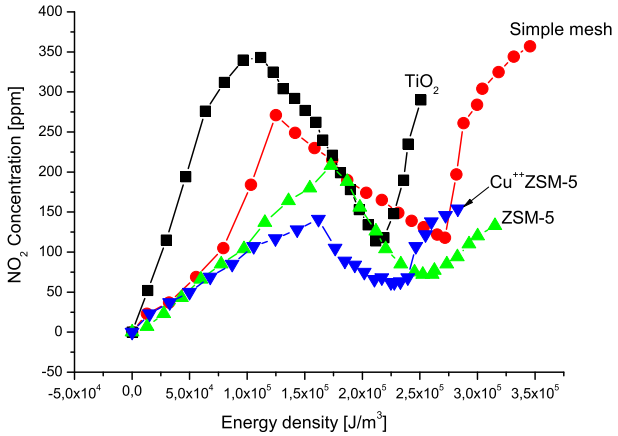

Fig. 5. (Color online) Nitrogen dioxide concentration versus energy density for the discharge with the needle to the mesh electrodes; needle to the mesh electrodes with TiO_2; with ZSM-5, or with Cu^{++}ZSM-5. Needle negative, $d = 8.1$ mm, $Q = 1.8$ slm. $RH = 0.8\%$. Mass of TiO_2 globules $m = 0.7691$ g, mass of ZSM-5 $m = 0.5203$ g and mass of Cu^{++}ZSM-5 $m = 0.5398$ g.

globules on the mesh. In this case the mechanism of NO decomposition is mainly associated with its adsorption on the surface of this zeolite.

Finally the energy density of the onset of discharge poisoning is highest for the discharge with a simple mesh electrode only. In this case the dominant role in ozone and nitrogen oxides production play collisions processes triggered by energetic electrons produced by the discharge. This is a situation, which corresponds to classical mechanisms of ozone and nitrogen oxides production, which is in general features described by equations (1)–(6).

The fact that various catalysts affect in different ways also the processes of nitrogen dioxides production is manifested in Figure 5, which shows the dependence of nitrogen dioxide concentration versus energy density for the discharge with a simple mesh electrode and a mesh electrode with a layer of globules of TiO_2, ZSM-5 or Cu^{++}ZSM-5.

From this figure we can see, that in contrast to nitrogen monoxide the concentration of nitrogen dioxide has a non zero value even before the onset of discharge poisoning. This result is valid for the discharge with a simple mesh as well as for the discharge with each of the investigated catalysts.

The models of discharge ozone, nitrogen monoxide and dioxide production in presence of titanium dioxide TiO_2, ZSM-5 zeolite, or copper ion exchanged Cu^{++}ZSM-5 zeolite at present do not exist.

However dependences of ozone, nitrogen monoxide and dioxide concentrations versus energy density, which were obtained in our experiments for the discharge without any catalyst on the mesh, follow similar trends as dependences presented in the paper of Yagi and Tanaka [29] for the silent discharge in air fed ozonizers. This qualitative agreement confirms validity of our results even in the case with various catalysts on the mesh electrode.

4 Conclusions

In order to clarify the role of titanium dioxide TiO_2, ZSM-5 zeolite, or copper ion exchanged Cu^{++}ZSM-5 zeolite on the onset of discharge poisoning we have investigated the effect of these catalysts on the production of ozone, nitrogen monoxide and nitrogen dioxide for a dc hollow needle to mesh corona discharge enhanced by the flow of air through the needle electrode. Our findings can be summarized as follows:

- The onset of discharge poisoning for a discharge with a simple mesh and also for a discharge with each of the investigated catalysts on the mesh coincides with the occurrence of nitrogen monoxide in the discharge products.
- The onset of discharge poisoning occurs at the highest energy density for the discharge with a simple mesh electrode.
- Placing the globules of any of the investigated catalysts on the mesh decreases the energy density of the onset of discharge poisoning.
- The energy density of the onset of discharge poisoning is smallest for the discharge with a layer of TiO_2 globules on the mesh.

The phenomenon of discharge poisoning plays an important role, which limits performance of ozone generating devices from air. Though our experiments were performed with the dc corona discharge the results dealing with the effect of investigated catalysts on discharge poisoning could also be used for other types of discharge energization or other electrode configurations.

This research has been supported by a Czech Science Foundation grant under contract No. 202/09/0176. The author would also like to express his thanks to Dr. Hyun-Ha Kim for valuable comments concerning ozone generation and catalysts activation.

References

1. B.L. Loeb, Ozone: Sci. Eng. **30**, 379 (2009)
2. K. Schmidt-Szalowski, Ozone: Sci. Eng. **18**, 41 (1996)
3. P. Martinez, D.K. Brandvold, Atmos. Environ. **30**, 4177 (1996)
4. N. Rehbein, V. Cooray, J. Electrostat. **51-52**, 333 (2001)
5. U. Kogelschatz, B. Eliasson, M. Hirth, Ozone: Sci. Eng. **30**, 367 (1988)
6. E.M. Van Veldhuizen, *Electrical discharges for environmental purposes: Fundamentals and Applications* (Nova Science Publishers, Inc., New York, 1999)
7. H. Weidong, R. Tingting, X. Weidong, Ozone: Sci. Eng. **29**, 107 (2007)
8. J.D. Moon, S.T. Geum, G.T. Lee, J. Korean Phys. Soc. **38**, 680 (2001)
9. J.D. Moon, J.S. Jung, J. Electrostat. **65**, 660 (2007)
10. J.S. Jung, J.D. Moon, J. Electrostat. **66**, 335 (2008)

11. R.B. Sun, Z.G. Xi, F.H. Chao, W. Zhang, H.S. Zhang, D.F. Yang, Atmos. Environ. **41**, 6853 (2007)
12. J. Van Durme, J. Dewulf, W. Sysmans, C. Leys, H. Van Langenhove, Appl. Catal. B Environ. **74**, 161 (2007)
13. J. Zhang, M. Minagawa, M. Matsuoka, H. Yamashita, M. Anpo, Catal. Lett. **66**, 241 (2000)
14. M. Iwamoto, S. Yokoo, K. Sakai, S. Kagawa, J. Chem. Soc. Farad. Trans. **77**, 1629 (1981)
15. M. Shelef, Catal. Lett. **15**, 305 (1992)
16. N. Goto, S. Kudo, H. Motoyama, S. Ohyama, Jpn J. Appl. Phys. **41**, L64 (2002)
17. A.W. Aylor, S.C. Larsen, J.A. Reimer, A.T. Bell, J. Catal. **157**, 592 (1995)
18. M. Anpo, M. Matsuoka, Y. Shioya, H. Yamashita, M. Che, H.H. Patterson, S. Weber, S. Ouellette, M.A. Fox, J. Phys. Chem. **98**, 5744 (1994)
19. M. Anpo, M. Matsuoka, H. Yamashita, W.S. Ju, S.E. Park, Y.G. Shul, J. Ind. Eng. Chem. **6**, 133 (2000)
20. K. Ebitani, M. Morokuma, J.H. Kim, A. Morikawa, J. Chem. Soc., Faraday Trans. **90**, 377 (1994)
21. J.S. Chang, IEEE Trans. Commun. **E79**, B 447 (1996)
22. S. Pekárek, V. Køíha, M. Šimek, R. Bálek, F. Hanitz, Plasma Source. Sci. Technol. **8**, 513 (1999)
23. Yu. Akishev, M. Grushin, I. Kochetov, V. Karalnik, A. Napartovich, N. Trushkin, Plasma Source. Sci. Technol. **14**, S18 (2005)
24. S. Pekárek, Eur. Phys. J. D **50**, 171 (2008)
25. F. Grum, L.F. Costa, Appl. Opt. **15**, 76 (1976)
26. J. Van Durme, J, Dewulf, Ch. Leys, H. Van Langenhove, Appl. Catal. B Environ. **78**, 324 (2008)
27. K.H. Becker, U. Kogelschatz, K.H. Schoenbach, R.J. Barker, *Non-equilibrium air plasmas at atmospheric pressure* (IoP, Bristol and Philadelphia, 2005)
28. T. Sano, N. Negishi, E. Sakai, S. Matsuzawa, J. Mol. Catal. A Chemistry **245**, 235 (2006)
29. S. Yagi, M. Tanaka, J. Phys. D **12**, 1509 (1979)